

Green's function Zero and Symmetric Mass Generation

Yichen Xu¹ and Cenke Xu¹

¹*Department of Physics, University of California, Santa Barbara, CA 93106, USA*

It is known that, under short-range interactions many topological superconductors (TSC) and topological insulators (TI) are trivialized, which means the boundary state of the system can be trivially gapped out by interaction without leading to symmetry breaking or topological ground state degeneracy. This phenomenon is also referred to as “symmetric mass generation” (SMG), and has attracted broad attentions from both the condensed matter and high energy physics communities. However, after the trivialization caused by interaction, some trace of the nontrivial topology of the system still persists. Previous studies have indicated that interacting topological TSC and TI could be related to the “zero” of Green's function, namely the fermion Green's function $G(i\omega \rightarrow 0) = 0$. In this work, through the general “decorated defect” construction of symmetry protected topological (SPT) states, we demonstrate the existence of Green's function zero after SMG, by mapping the evaluation of the Green's function to the problem of a single particle path integral. This method can be extended to the cases without spatial translation symmetry, where the momentum space which hosts many quantized topological numbers is no longer meaningful. Using the same method one can demonstrate the existence of the Green's function zero at the “avoided topological transition” in the bulk of the system.

PACS numbers:

I. INTRODUCTION

Short range interactions can modify the classification of topological superconductors (TSC) and topological insulators (TI) in the classic “ten-fold way” table for free electrons¹⁻³. The most prominent feature of a TSC or a TI is at its boundary, i.e in the noninteracting limit, the boundary of a TSC or TI should be gapless unless the boundary breaks the defining symmetry of the system. A short range interaction can enrich the phenomena at the boundary of a TSC and TI: it can drive the boundary into a spontaneous symmetry breaking phase, or a gapped topological phase which preserves all the symmetries⁴⁻⁷. But it has also been realized that, a short range interaction may trivialize some of the TSCs and TIs, in the sense that short range interaction can “trivially” gap out the boundary of some TSCs and TIs without breaking any symmetry or leading to any ground state degeneracy. The first $1d$ example of this interaction-trivialized TSC was found in Ref. 8,9, and soon other examples were found in all dimensions^{6,10-18}. For example, now it is known that 16 copies of the TSC ³He-B phase is trivialized by interaction, hence although this TSC in the noninteracting limit has a \mathbb{Z} classification, under interaction ³He-B has a \mathbb{Z}_{16} classification^{6,13}.

Interaction trivialized TSC and TI has a deep relation with another phenomenon called “symmetric mass generation” (SMG). In the noninteracting limit the boundary of a $(d + 1)$ -dimensional TSC is described by a d -dimensional gapless Majorana fermion (or chiral Majorana fermion depending on the dimensionality), which carries with it certain 't Hooft anomaly of the defining symmetries of the TSC. A mass term of the boundary fermion will explicitly break the symmetry, and hence is prohibited to exist. When interaction reduces the classification of a TSC from \mathbb{Z} to \mathbb{Z}_N , it means that for N copies

of the d -dimensional Majorana fermions, it is possible to generate a gap through interaction without any degeneracy at the d -dimensional boundary, and the expectation value of any fermion bilinear mass operator is zero. The mechanism of SMG is in stark contrast with the ordinary mass generation of a Dirac or Majorana fermion (the well-known Gross-Neveu-Yukawa-Higgs mechanism¹⁹), which is caused by the condensation of a boson that couples to the fermion bilinear mass term. The condensation of the boson will break the symmetry of the system, and lead to a nonzero expectation value of a fermion mass term. The SMG has attracted broad attentions from both the condensed matter²⁰⁻²³ and high energy communities²⁴⁻³¹ in the last few years, partly motivated by the observation that the SMG mechanism may be related to the lattice regularization of chiral gauge theories such as the Grand Unified Theories³²⁻³⁹.

A natural question one may ask is that, after the interaction “trivializes” the system, or after the SMG, is there still any remaining trace of the nontrivial topology of the original noninteracting system? Or for a system with a fully gapped spectrum, how do we know the gap originates from the mechanism of SMG? The two most important features of TSCs or TIs are their stable boundary states, and the unavoidable bulk topological phase transition from the trivial insulator. When a TSC or TI is trivialized by interaction, both features mentioned above no longer robustly hold. It has been proposed before that strongly interacting TIs and TSCs may have a close relation with the zero of fermion Green's functions^{20,22,23,28,40-43}. In this work we use the general “decorated defect” construction of symmetry protected topological (SPT) states⁴⁴, and map the computation of the fermion Green's function to a problem of single particle path integral. Our method demonstrates in arbitrary dimensions the existence of fermion Green's function zero,

after the interaction trivializes the TSC and TI, i.e. after the symmetric mass generation. One of the arguments (which will be reviewed later) for the existence of the Green's function zero relies on the quantized topological number defined with fermion Green's function in the momentum space. Our method can be generalized to the cases without translation symmetry, where a momentum space is no longer meaningful.

II. GREEN'S FUNCTION "ZERO" FROM DECORATED DEFECTS

Intuitively the decorated defect construction of a SPT state follows three steps: (1) one starts with a bosonic system with certain symmetry G , and drive the bosonic system into an ordered state with spontaneous symmetry breaking of the symmetry G , which allows topological defects; (2) decorate the topological defects with a lower dimensional SPT state, and (3) eventually proliferate the defects to restore the symmetry G . This decorated defect construction was originally designed for bosonic SPT states⁴⁴, but it also applies to fermionic TSCs and TIs. For example, the $2d$ TSC with the $Z_2 \times Z_2^T$ symmetry ($p \pm ip$ TSC) can be constructed by decorating the Z_2 domain wall with a $1d$ TSC with the time-reversal (Z_2^T) symmetry (the $1d$ BDI class TSC or the so called Kitaev's chain); The $3d$ TSC (or TI) of the AIII class can be constructed by decorating a $U(1)$ vortex line with the Kitaev's chain.

We will start with the example of $2d$ TSC with $Z_2 \times Z_2^T$ symmetry, and first compute the fermion Green's function at the $1d$ boundary of the system. Consider a $2d$ Ising magnet in a ferromagnetic phase (SSB of the Z_2 spin symmetry). We perform the "decorated domain wall" construction by decorating each Ising domain wall with a $1d$ Kitaev chain with time-reversal symmetry Z_2^T . The parameters of the Hamiltonian are then tuned to proliferate these decorated domain walls. When a $1d$ Z_2 domain wall meets (or intersect) with the $1d$ boundary of the system, the domain wall becomes a $0d$ object decorated with Majorana zero modes coming from the boundary of the Kitaev's chain. These Majorana zero modes transform under the time-reversal Z_2^T as $\gamma_a \rightarrow \gamma_a$, hence any Hermitian fermion bilinear operator $i\gamma_a\gamma_b$ would break the time-reversal symmetry and hence prohibited. For decoration number $\nu = 8$, with a proper flavor symmetry between the Majorana fermion operators γ_a , the interaction will induce a many-body symmetric gap between the Majorana modes, and drive the fermion Green's function at each $0d$ intersection to the following form^{20,43}:

$$G_{ab}(i\omega) \sim \frac{i\omega\delta_{ab}}{(i\omega)^2 - m^2}, \quad (1)$$

in which m is proportional to the strength of the fermion interaction. There is a uniform gap energy scale in the Green's function, as long as the eight Majorana fermion

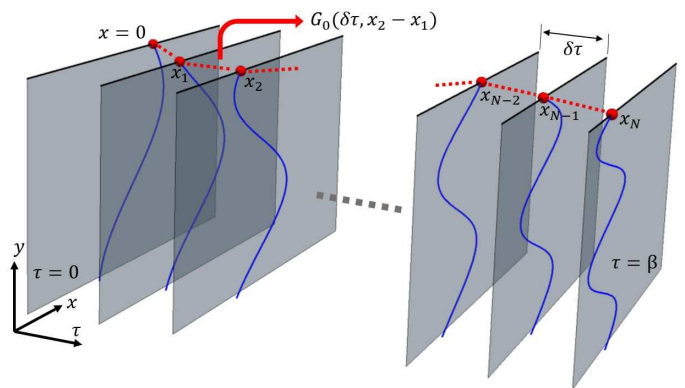


FIG. 1: Physical picture of the path integral in Eq. 3. Here each plane represents the $2d$ bulk at an intermediate time, the solid lines are the decorated domain walls, the circles are gapped Majorana modes at the boundary. The Majorana modes are connected by dashed lines, which stand for the local Green's function $G_0(\delta\tau, x_i - x_{i-1})$.

operators γ_a form an irreducible representation of the flavor symmetry, such as a spinor representation of $SO(7)$ or $SO(5)$. G_{ab} approaches zero when $\omega \rightarrow 0$. Notice that this Green's function takes a different form from a free massive $0d$ fermion, where a mass term would explicitly break the time-reversal.

After being gapped by interaction through the SMG, in the Euclidean time the Majorana modes (MM) Green's function reads

$$G_{ab}(\tau) = G_{MM}(\tau)\delta_{ab} \sim \text{sgn}(\tau)e^{-m|\tau|}\delta_{ab}. \quad (2)$$

Our goal is to compute the fermion Green's function after the proliferation of Ising domain wall. To do this we map the computation of the Green's function to the following Feynmann path-integral problem in the $(1+1)d$ space-time, and the different choice of path $x(\tau)$ physically represents the fluctuation of the domain wall configuration:

$$G_{ab}(\beta, x) = \delta_{ab}G(\beta, x),$$

$$G(\beta, x) \sim \text{sgn}(\beta) \int D[x(\tau)] \prod_{i=1}^N G_0(\delta\tau, \delta x_i) \rho(\delta\tau, \delta x_i), \quad (3)$$

Where $\delta x_i = x_i - x_{i-1}$. Here we have inserted $N-1$ intermediate steps between the starting point ($\tau = 0, x_0 = 0$) and the end point ($\tau = \beta, x_N = x$). x_i is the spatial coordinate along the $1d$ boundary space with lattice constant a (Fig. 1). $\delta\tau = \frac{|\beta|}{N}$ is the time interval for each intermediate step.

The physical picture behind Eq. 3 is shown in Fig. 1. $D[x(\tau)] \sim \prod_{i=1}^{N-1} (dx_i/a)$ is the integral measure of Feynmann path integral, which should arise from summing over x_i along the $1d$ space with lattice constant a : $\sum_x f(x) = \frac{1}{a} \int dx f(x)$. $G_0(\delta\tau, \delta x) = e^{-m\sqrt{\delta\tau^2 + \delta x^2}}$ is the intermediate step short range propagation of the MM,

inherited from Eq. 2. Here we take the simplest possible form of $G_0(\delta\tau, \delta x)$ as a generalization of Eq. 2, which has a Lorentz invariance between $\delta\tau$ and δx . $\rho(\delta\tau, \delta x_i)$ with $\delta x_i = x_i - x_{i-1}$ is an extra factor to control the fluctuation between intermediate steps, whose form depends on the microscopic details of domain wall proliferation. We will first consider the simplest scenario with $\rho(\delta\tau, \delta x_i) = 1$.

A direct path integral of Eq. 3 is a bit awkward. We could change the variables inside each Green's function using the following trick:

$$G(\beta, x) = \text{sgn}(\beta) \int D[x(\tau)] \prod_{i=1}^N \frac{d\lambda_i d\phi_i}{2\pi} \prod_{j=1}^N G_0(\delta\tau, \phi_j) \times \exp\left(i \sum_{k=1}^N \lambda_k (x_k - x_{k-1} - \phi_k)\right). \quad (4)$$

Here we introduced two sets of auxiliary variables: λ_i are Lagrangian multipliers; ϕ_i substitute the coordinate differences. Now we can integrate out $x(\tau)$ first, which generates a product of delta functions $\prod_{i=2}^N \delta(\lambda_i - \lambda_{i-1})$, i.e. all λ_i should equal. Then we can further integrate out λ_i ,

$$G(\beta, x) = \text{sgn}(\beta) \left(\frac{1}{a}\right)^{N-1} \int \prod_{i=1}^N d\phi_i G_0(\delta\tau, \phi_i) \times \delta\left(x - \sum_{k=1}^N \phi_k\right). \quad (5)$$

Now we can perform a Fourier transformation of the spatial coordinate x , and

$$G(\beta, k) \sim \frac{1}{a} \int dx e^{ikx} G(\beta, x) = \text{sgn}(\beta) \left(\frac{1}{a} \int d\phi e^{ik\phi} G_0(\delta\tau, \phi)\right)^{\frac{|\beta|}{\delta\tau}}. \quad (6)$$

Here we have replace all N in the expression by $|\beta|/\delta\tau$, and view $\delta\tau$ as an independent variable, unrelated to β . $G(\beta, k)$ takes an exponential form just like $G_{\text{MM}}(\tau)$, and this comparison allows us to define an effective mass gap for $G(\beta, k)$ as follows

$$m'(k) \equiv -\frac{\ln\left(\frac{1}{a} \int d\phi e^{ik\phi} G_0(\delta\tau, \phi)\right)}{\delta\tau} = -\frac{\ln\left(\frac{2m\delta\tau}{a\sqrt{m^2+k^2}} K_1(\delta\tau\sqrt{m^2+k^2})\right)}{\delta\tau}, \quad (7)$$

so that $G(\beta, k) \sim \text{sgn}(\beta) e^{-m'(k)|\beta|}$. $K_1(x)$ is the modified Bessel function of the second kind.

With large m or k , the effective mass $m'(k)$ is proportional to $m'(k) \sim \sqrt{m^2+k^2}$. Hence with large m, k in the momentum and Matsubara frequency space, the fermion Green's function takes the approximate form

$$G(i\omega, k) \sim \frac{i\omega}{\omega^2 + m^2 + k^2}. \quad (8)$$

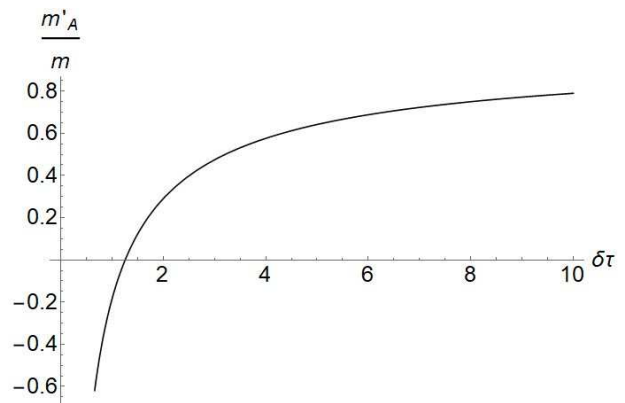


FIG. 2: Effective mass gap ratio $m'(0)/m$ as a function of $\delta\tau$. The sign of $m'(0)$ changes from positive to negative while decreasing $\delta\tau$, suggesting a phase transition caused by domain wall fluctuation. Here we set $m = a = 1$.

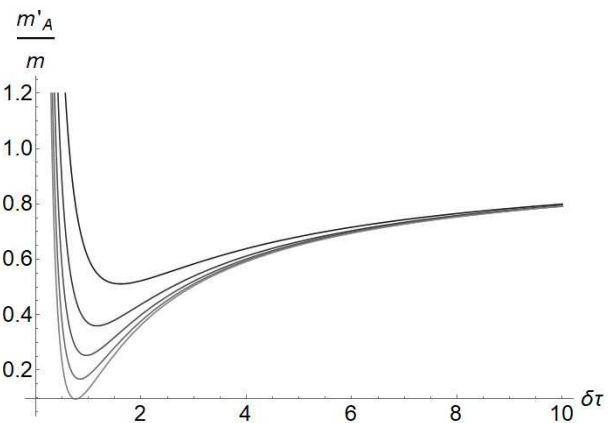


FIG. 3: Effective mass ratio versus $\delta\tau$ for different control parameter A with $m = a = 1$. From top to bottom $A = 1, 2, \dots, 5$.

This form of Green's function after SMG is consistent with the fermion Green's functions obtained in different models^{20,22,23,28,43}, after taking the trace of the Green's functions in these literature, since in our formalism there is a single component of Majorana fermion in the Dirac space. As long as $m'(k) > 0$, i.e. the fermion Green's function decays exponentially in the long time limit, the Fourier transformation of the Green's function to the Matsubara frequency space will have zero at $\omega = 0$.

The ratio between effective mass gap $m'(0)$ and m as a function of $\delta\tau$ is shown in Fig. 2, in which we set $m = a = 1$. When $\delta\tau \ll a$ (meaning there are many intervals in the path integral), the effective mass m' becomes negative, this means that in the long time limit the Green's function of the Majorana fermion no longer exponentially decays. The sign change of m' signals a phase transition, which is caused by increased steps of intervals, or physically stronger fluctuation of the domain wall.

Now we turn on the control function $\rho(\delta\tau, \delta x_i)$ in the Green's function path integral. For example, we can turn

on a Gaussian control function of the fluctuation of the domain wall: $\rho_A(\delta\tau, \delta x_i) = \exp(-(\delta x_i/\delta\tau)^2/A)$, It is not hard to see, from Eqs. 4 to 7, that adding such control factor will not alter the exponential form of the outcome, while the effective mass gap now reads

$$m'_A = -\frac{\ln\left(\frac{1}{a} \int d\phi G_0(\delta\tau, \phi) e^{-\phi^2/(A\delta\tau^2)}\right)}{\delta\tau}. \quad (9)$$

Results of numerical integral of ϕ with different A are plotted in Fig. 3. Again all m'_A approaches to m when $\delta\tau \rightarrow \infty$. And as expected, smaller A will lead to a larger m' , because a smaller A suppresses proliferation of the domain walls more strongly.

III. HIGHER SPATIAL DIMENSIONS

“Decorated defect construction” of TSCs and TIs, or more generally SPT states can be generalized to higher dimension. As we mentioned in the introduction, the $3d$ TI in the AIII class can be constructed by starting with a superfluid with spontaneous U(1) symmetry breaking in the $3d$ bulk, then decorate each vortex line with a Kitaev’s chain, and eventually proliferate the vortex line to restore the U(1) symmetry in the bulk. A $4d$ TSC with SO(3) and time-reversal symmetry can be constructed in a similar way: in the $4d$ space, the hedgehog monopole of a SO(3) vector order parameter is a line defect; one can start with an ordered phase with a SO(3) vector order parameter, and decorate the hedgehog monopole line with a $1d$ Kitaev’s chain, and then eventually proliferate the monopole line.

In general one can start with a d -dimensional system with symmetry group G (for example SO($d-1$)) that allows one dimensional topological defect line. In this case each defect line could be decorated with Kitaev chains, and when these line defects are proliferated we again presumably obtain gapped TSC with symmetry $G \times Z_2^T$. When the decorated line defects meet the ($d-1$)-dimensional boundary, the $0d$ intersection is decorated with Majorana zero modes. When eight copies of Kitaev’s chains are decorated on the $1d$ defect line, the Majorana modes at the intersection is gapped by interaction through the SMG mechanism, and their Green’s function is given by Eq. 1.

Once we proliferate the defects, the fermion Green’s function at the ($d-1$)-dimensional boundary can still reduce to a path integral problem:

$$G^{(d-1)}(\beta, \mathbf{x}) = \text{sgn}(\beta) \int D[\mathbf{x}(\tau)] \prod_{i=1}^N G_0^{(d-1)}(\delta\tau, \delta\mathbf{x}_i) \times \rho(\delta\tau, \delta\mathbf{x}_i) \quad (10)$$

where $\delta\mathbf{x}_i = \mathbf{x}_i - \mathbf{x}_{i-1}$, and \mathbf{x}_i are intermediate positions at the $d-1$ dimensional boundary (with $\mathbf{x}_0 = 0$ and $\mathbf{x}_N = \mathbf{x}$) and $G_0^{(d-1)}(\delta\tau, \delta\mathbf{x}_i) = \exp\left(-m\sqrt{\delta\tau^2 + \delta\mathbf{x}_i^2}\right)$ is

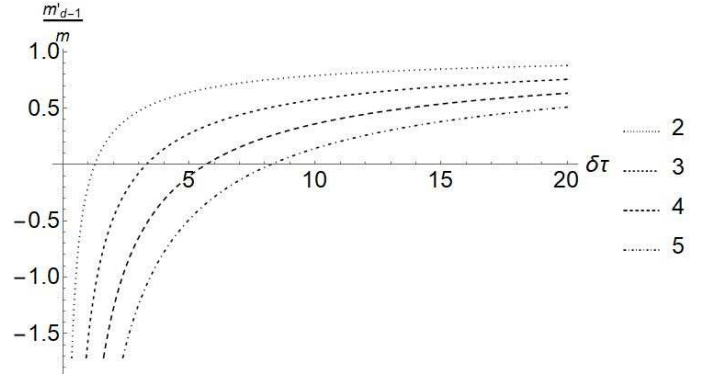


FIG. 4: m'_{d-1}/m as functions of $\delta\tau$ with $m = a = 1$. From top to bottom $d = 2, 3, 4, 5$.

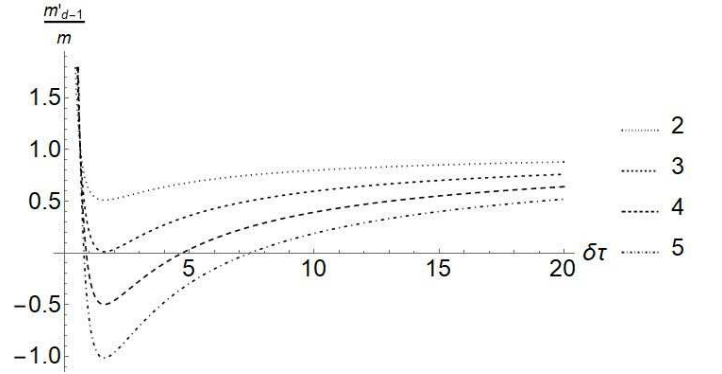


FIG. 5: m'_{d-1}/m under Gaussian control function as functions of $\delta\tau$, with $m = a = 1$, $d = 2$ to 5 and $A = 1$.

the simplest extension of Eq. 1 to ($d-1$)-dimensional space. The same trick of variable substitution applies here:

$$G^{(d-1)}(\beta, \mathbf{x}) = \text{sgn}(\beta) \int D[\mathbf{x}(\tau)] \prod_{i=1}^N \frac{d\vec{\lambda}_i d\vec{\phi}_i}{(2\pi)^{d-1}} \times G_0^{(d-1)}(\delta\tau, \vec{\phi}_i) \rho(\vec{\phi}_i) \exp\left(i \sum_{k=1}^N \vec{\lambda}_k \cdot (\mathbf{x}_k - \mathbf{x}_{k-1} - \vec{\phi}_k)\right). \quad (11)$$

Again, integrating out $\mathbf{x}(t)$ and $\vec{\lambda}_i$ leaves us with a single constraint $\delta^{(d)}(\mathbf{x} - \sum_{i=1}^N \vec{\phi}_i)$. After integrating over \mathbf{x} , we are left with $\int d\mathbf{x} G^{(d-1)}(\beta, \mathbf{x}) \propto \text{sgn}(\beta) e^{-m'_{d-1}|\beta|}$, in which

$$m'_{d-1} \equiv -\frac{1}{\delta\tau} \ln \left\{ \left(\frac{1}{a}\right)^{d-1} \int d^{d-1}\vec{\phi} \times G_0^{(d-1)}(\delta\tau, \vec{\phi}) \rho(\vec{\phi}) \right\} = -\frac{\ln\left(\frac{ma}{\pi} \left(\frac{2\pi\delta\tau}{ma^2}\right)^{\frac{d}{2}} K_{d/2}(m\delta\tau)\right)}{\delta\tau} \quad (\text{for } \rho(\vec{\phi}) = 1) \quad (12)$$

is the new effective mass gap. The ratios between m'_{d-1} and m is plotted in Fig. 4, and we can see from the

plot that increasing spatial dimension makes the effective mass gap smaller, indicating that fluctuation is stronger for higher dimensions. Indeed, for higher dimensions there is more space for the proliferation of path $\mathbf{x}(\tau)$. When the Gaussian control function $\rho_A(\delta\tau, \delta\mathbf{x}_i) = \exp(-(\delta\mathbf{x}_i/\delta\tau)^2/A)$ is turned on, the stronger fluctuation for higher dimensions makes the Gaussian suppression less effective (see Fig. 5). Nevertheless, for nonzero A , m'_{d-1} can still be positive (and hence there is a zero in the Green's function) for a broad range of parameters.

IV. SCENARIOS WITHOUT TRANSLATION SYMMETRY

One of the previous observations and arguments for the existence of fermion Green's function zero, is based on the quantized topological number for TSC and TI defined with the fermion Green's function^{40,41}. A typical topological number can be defined in the Matsubara frequency and momentum space of the Euclidean space-time fermion Green's function⁴⁵⁻⁴⁹: $n \sim \int d\omega d^d k \text{tr}[B(G^{-1}\partial G) \wedge (G^{-1}\partial G) \cdots]$, where G is the matrix of the fermion Green's function, and B is a matrix in the flavor space. The number n must be a quantized integer mathematically, and it can only change when the Green's function has singularity.

The number n can change through two types of "transitions". The first type of transition is a physical transition where $G^{-1}(i\omega = 0)$ vanishing to zero at certain momentum, i.e. the fermions become gapless. In this case the physical topological transition coincides with the transition of the topological number. However, one can easily notice that in the definition of n , G^{-1} and G are on an equal footing, hence theoretically the topological number mentioned above can also change when $G(i\omega = 0) = 0$, i.e. when the Green's function has a zero. Hence when the TSC or TI is trivialized by the interaction, although there is no unavoidable phase transition between the TSC (or TI) and a trivial insulator, the topological number n still has to change discontinuously somewhere in the phase diagram, and since there is no real physical transition, the number n has to change through zero of the Green's function.

This argument for Green's function zeros relies on the quantized topological number in the momentum space, hence it requires the translation symmetry. But none of the TSC and TI in the "ten-fold way" classification requires translation symmetry, hence it is natural to ask whether the Green's function zeros persist when the translation symmetry is broken. Normally the translation symmetry breaking is caused by disorder, i.e. a random potential energy. But a fermion bilinear potential term $i\gamma_a\gamma_b$ breaks the time-reversal symmetry of the decorated Kitaev's chain. Hence the most natural translation symmetry breaking perturbation that can be turned on in the system, is a spatial dependent random four-fermion interaction, i.e. a randomized $m(x)$ in Eq. 2,

Eq. 3.

Now Eq. 3 is modified to

$$G(\beta, x) = \text{sgn}(\beta) \int D[x(\tau)] e^{\sum_{i=1}^N -m(x_i)\sqrt{\delta\tau^2+\delta x_i^2}} \rho_A(\delta\tau, \delta x_i). \quad (13)$$

$m(x_i)$ is a space-dependent but time-independent function. In principle $m(x_i)$ could be any function of space. Here we focus on the situation when $m(x_i) = m + \delta m(x_i)$, where m is a positive constant, while $\delta m(x_i)$ is random function of space with zero mean and Gaussian distribution. After disorder average, the expression for the Green's function is

$$\begin{aligned} \overline{G(\beta)} &= \text{sgn}(\beta) \int D[x(\tau)] \\ &e^{\sum_{i=1}^N -m\sqrt{\delta\tau^2+\delta x_i^2} + \sum_{j,k} \Delta\delta(x_j-x_k)\sqrt{\delta\tau^2+\delta x_j^2}\sqrt{\delta\tau^2+\delta x_k^2}} \\ &\times \rho_A(\delta\tau, \delta x_i). \end{aligned} \quad (14)$$

Δ is given by the Gaussian distribution of $\delta m(x_i)$:

$$\overline{\delta m(x_j)\delta m(x_k)} \sim \Delta\delta(x_j-x_k). \quad (15)$$

The delta function $\delta(x_j-x_k)$ is only nonzero when $x_j=x_k$. This condition automatically satisfies when $j=k$, but may still happen when $j \neq k$, meaning the path $x(\tau)$ returns to the same spatial location at different time instances. We first consider the contribution from disorder average when $j=k$:

$$\begin{aligned} \overline{G(\beta)}_0 &= \text{sgn}(\beta) \int D[x(\tau)] e^{\sum_{i=1}^N -m\sqrt{\delta\tau^2+\delta x_i^2} + \sum_i \Delta(\delta\tau^2+\delta x_i^2)} \\ &\times \rho_A(\delta\tau, \delta x_i). \\ &= \text{sgn}(\beta) \exp(-\beta(m'_{\tilde{A}} - \Delta\delta\tau)). \end{aligned} \quad (16)$$

Here $m'_{\tilde{A}}$ with $\tilde{A} = \frac{A}{1-A\Delta}$ is the effective mass gap defined in Eq. 9 with a new Gaussian control parameter $\tilde{A} = \frac{A}{1-A\Delta}$. Thus $\overline{G(\beta)}_0$ behaves identically to the previously computed Gaussian suppressed Green's function, albeit with a slower decaying rate, $m_{A,\Delta}^{(2)} \equiv m'_{\tilde{A}} - \Delta\delta\tau$. The effect of disorder on the effective mass $m_{A,\Delta}^{(2)}$ is plotted in Fig. 6.

For the contribution from $j \neq k$ (we assume that $j < k$ hereafter), we can expand the Green's function into powers of Δ . The first order of this expansion is

$$\begin{aligned} \overline{G(\beta)}_1 &\equiv \Delta \text{sgn}(\beta) e^{\beta\Delta\delta\tau} \sum_{j \neq k} \int D[x(\tau)] e^{\sum_{i=1}^N -m\sqrt{\delta\tau^2+\delta x_i^2}} \\ &\times \sum_{j \neq k} \delta(x_j-x_k) \sqrt{\delta\tau^2+\delta x_j^2} \sqrt{\delta\tau^2+\delta x_k^2} \\ &\times \prod_{i=1}^N \rho_{\tilde{A}}(\delta\tau, \delta x_i). \end{aligned} \quad (17)$$

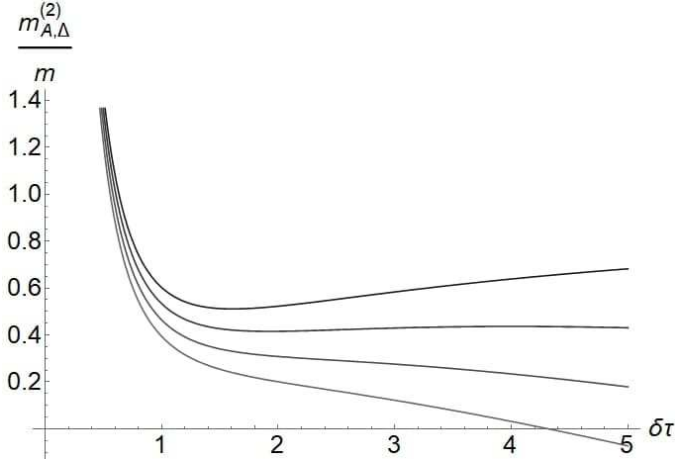


FIG. 6: Effective mass gaps $m_{A,\Delta}^{(2)}$ for the lowest order of disorder averaged Green's function $\overline{G(\beta)_0}$ as functions of $\delta\tau$. Here we set $m = a = A = 1$, $\Delta = 0, 0.05, 0.1, 0.15$ from the top to bottom.

Again using the previous variable substitution, we obtain

$$\begin{aligned} \overline{G(\beta)_1} &= \Delta \text{sgn}(\beta) e^{\beta\Delta\delta\tau} \sum_{j \neq k} \int D[x(\tau)] \prod_{i=1}^N \frac{d\lambda_i d\phi_i}{2\pi} \\ &\times e^{-\sum_i m \sqrt{\delta\tau^2 + \phi_i^2} - i\lambda_i(x_i - x_{i-1} - \phi_i)} \delta(x_j - x_k) \\ &\times \sqrt{\delta\tau^2 + \phi_j^2} \sqrt{\delta\tau^2 + \phi_k^2} \prod_{i=1}^N \rho_{\tilde{A}}(\delta\tau, \phi_i). \end{aligned} \quad (18)$$

Integrating over all x_i and x_0 , we obtain the product of a series of delta functions

$$\begin{aligned} &\prod_{i=1}^{j-1} \delta(\lambda_i - \lambda_{i+1}) \prod_{i=j+1}^{k-1} \delta(\lambda_i - \lambda_{i+1}) \prod_{i=k+1}^{N-1} \delta(\lambda_i - \lambda_{i+1}) \\ &\times \delta(\lambda_N) \delta(\lambda_k - \lambda_{k+1} + \lambda_j - \lambda_{j+1}). \end{aligned} \quad (19)$$

For example $\delta(\lambda_N)$ comes from $\int dx_N$. Integrating out other x_i will enforce $\lambda_i = 0$ for all $i > k$; $\lambda_i = \lambda_1$ for all $i \leq j$; and $\lambda_i = \lambda_k$ for all $j < i \leq k$. The final delta function above thus also enforces $\lambda_i = \lambda_1 = 0$ with all $i \leq j$. Notice that λ_k is unconstrained here, because $\delta(x_j - x_k)$ effectively removes one δ function constraint for λ_i 's. So we are left with the a single integral of $\lambda_k \equiv \lambda$, and the result is

$$\begin{aligned} \overline{G(\beta)_1} &= 2\Delta \text{sgn}(\beta) e^{\beta\Delta\delta\tau} \sum_{j < k} (\tilde{G}_\Delta(0))^{N-(k-j)-1} \partial_m \tilde{G}_\Delta(0) \\ &\times \int d\lambda (\tilde{G}_\Delta(\lambda))^{k-j-1} \partial_m \tilde{G}_\Delta(\lambda) \\ &= \overline{G(\beta)_0} \times 2\Delta \frac{\partial_m \tilde{G}_\Delta(0)}{\tilde{G}_\Delta(0)} \sum_{h=1}^{N-1} (N-h) \\ &\times \int d\lambda \left(\frac{\tilde{G}_\Delta(\lambda)}{\tilde{G}_\Delta(0)} \right)^{h-1} \frac{\partial_m \tilde{G}_\Delta(\lambda)}{\tilde{G}_\Delta(0)}. \end{aligned} \quad (20)$$

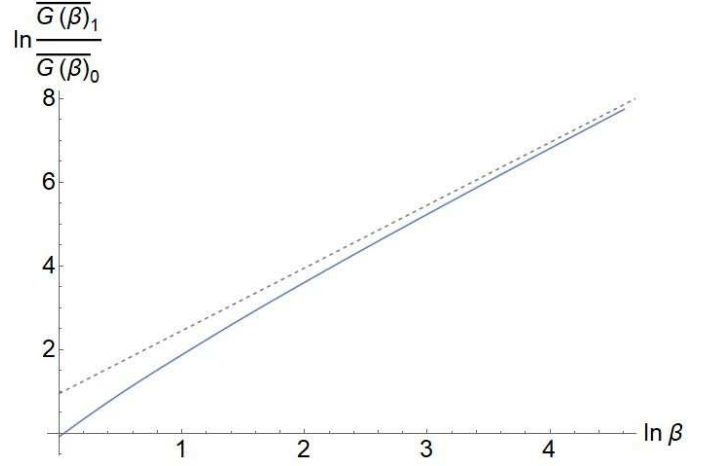


FIG. 7: Log-log plot of numerical integration of $\overline{G(\beta)_1}/\overline{G(\beta)_0}$. Here we set $m = a = A = 1$, $\delta\tau = 0.3$ and $\Delta = 0.1$. The dashed line is a guide to the eye with slope $3/2$.

Here $\tilde{G}_\Delta(\lambda) = \int \frac{d\phi}{a} e^{i\lambda\phi - m\sqrt{\delta\tau^2 + \phi^2}} \rho_{\tilde{A}}(\delta\tau, \phi)$.

Numerical integration of λ in the expression above shows that the ratio between the first two orders of the Δ expansion, i.e. $\overline{G(\beta)_1}/\overline{G(\beta)_0}$ approaches $\beta^{3/2}$ for large β (see Fig. 7). Thus at large β the overall behavior of the first order term in the Δ expansion still exponentially decays with β . The behavior of large β can be understood in the following way: The integral of $\tilde{G}_\Delta(\lambda)$ can be approximated by replacing $\sqrt{\delta\tau^2 + \phi^2}$ by $\delta\tau + |\phi|$ in the exponent, which means $\frac{\tilde{G}_\Delta(\lambda)}{\tilde{G}_\Delta(0)}$ and $\frac{\partial_m \tilde{G}_\Delta(\lambda)}{\tilde{G}_\Delta(0)}$ behaves approximately as $e^{-\frac{A}{4(1-A\Delta)}\lambda^2}$. The λ integral gives a $\frac{1}{\sqrt{h}}$ factor in each term of the summation of Eq. 20. Eventually $\overline{G(\beta)_1}/\overline{G(\beta)_0}$ is evaluated as

$$\sum_{h=1}^N \frac{N-h}{\sqrt{h}} \sim \int_0^\beta dx \frac{\beta-x}{\sqrt{x}} \sim \beta^{3/2}. \quad (21)$$

And as long as the overall behavior of $\overline{G(\beta)}$ decays exponentially with β , the Fourier transformation of $\overline{G(\beta)}$ has a zero at $\omega = 0$.

At higher dimensions, it is less likely for $\mathbf{x}_j = \mathbf{x}_k$ at $j \neq k$, i.e. it is less likely for a path $\mathbf{x}(\tau)$ to return to exactly the same spatial location at two different time instances. Hence we expect that for higher spatial dimensions the zeroth order $\overline{G(\beta)_0}$ in the formulation above should be even more accurate.

V. THE ‘‘AVOIDED’’ TOPOLOGICAL TRANSITION IN THE BULK

As we discussed in the introduction, besides the non-trivial boundary state, there is another prominent feature of a TI and TSC: there must be an unavoidable bulk topological transition between the TI or TSC and the

trivial insulator when tuning the parameter of the bulk Hamiltonian. However, once the TI or TSC is trivialized by interaction, not only can the boundary state be trivially gapped, the bulk topological transition also becomes avoidable^{8,9}: there is an adiabatic path in the phase diagram connecting the original TI (or TSC) phase and the original trivial insulator phase without closing the gap at all. In this case the original topological transition is also called “unnecessary transition”^{50,51}. In fact there is a close relation between the boundary state and the bulk topological transition. The simplest model to visualize such relation is the Chalker-Coddington model^{52,53}, which was first developed for the integer quantum Hall transition. This boundary-bulk relation can be made much more general for strongly interacting symmetry protected topological states⁵⁴. In general the bulk topological transition between the trivial phase and the SPT phase can be viewed as growing islands of the SPT phase

inside a trivial phase, and the unavoidable topological transition originates from the nontrivial interface states between the trivial and SPT phases. When the interfaces percolate, the bulk is at the topological transition. Using this picture, our real-space calculation for Green’s function in the previous sections for a d -dimensional boundary, also applies to the avoided bulk topological transition at d -dimensions.

— *Summary*

In this work we demonstrate the existence of the Green’s function zero as a remaining trace of nontrivial topology, after the system acquires a fully gapped spectrum after the mechanism of symmetric mass generation. Our method mostly relies on the real space decorated defect construction of the SPT states, and it does not require spatial symmetries such as translation.

This work is supported by NSF Grant No. DMR-1920434, and the Simons Foundation.

-
- ¹ A. P. Schnyder, S. Ryu, A. Furusaki, and A. W. W. Ludwig, AIP Conf. Proc. **1134**, 10 (2009).
- ² S. Ryu, A. Schnyder, A. Furusaki, and A. Ludwig, New J. Phys. **12**, 065010 (2010).
- ³ A. Kitaev, AIP Conf. Proc. **1134**, 22 (2009).
- ⁴ P. Bonderson, C. Nayak, and X.-L. Qi, Journal of Statistical Mechanics: Theory and Experiment **2013**, P09016 (2013), URL <http://stacks.iop.org/1742-5468/2013/i=09/a=P09016>.
- ⁵ C. Wang, A. C. Potter, and T. Senthil, Phys. Rev. B **88**, 115137 (2013), URL <https://link.aps.org/doi/10.1103/PhysRevB.88.115137>.
- ⁶ L. Fidkowski, X. Chen, and A. Vishwanath, Phys. Rev. X **3**, 041016 (2013), URL <https://link.aps.org/doi/10.1103/PhysRevX.3.041016>.
- ⁷ M. A. Metlitski, C. L. Kane, and M. P. A. Fisher, Phys. Rev. B **92**, 125111 (2015), URL <https://link.aps.org/doi/10.1103/PhysRevB.92.125111>.
- ⁸ L. Fidkowski and A. Kitaev, Phys. Rev. B **81**, 134509 (2010).
- ⁹ L. Fidkowski and A. Kitaev, Phys. Rev. B **83**, 075103 (2011).
- ¹⁰ X.-L. Qi, New J. Phys. **15**, 065002 (2013).
- ¹¹ H. Yao and S. Ryu, Phys. Rev. B **88**, 064507 (2013).
- ¹² S. Ryu and S.-C. Zhang, Phys. Rev. B **85**, 245132 (2012).
- ¹³ C. Wang and T. Senthil, Phys. Rev. B **89**, 195124 (2014).
- ¹⁴ Y.-Z. You and C. Xu, Phys. Rev. B **90**, 245120 (2014), URL <https://link.aps.org/doi/10.1103/PhysRevB.90.245120>.
- ¹⁵ H. Isobe and L. Fu, Phys. Rev. B **92**, 081304 (2015), URL <https://link.aps.org/doi/10.1103/PhysRevB.92.081304>.
- ¹⁶ H. Song, S.-J. Huang, L. Fu, and M. H. Hermele, Phys. Rev. X **7**, 011020 (2017), URL <https://link.aps.org/doi/10.1103/PhysRevX.7.011020>.
- ¹⁷ T. Morimoto, A. Furusaki, and C. Mudry, Phys. Rev. B **92**, 125104 (2015), URL <https://link.aps.org/doi/10.1103/PhysRevB.92.125104>.
- ¹⁸ E. Tang and X.-G. Wen, Phys. Rev. Lett. **109**, 096403 (2012), URL <https://link.aps.org/doi/10.1103/PhysRevLett.109.096403>.
- ¹⁹ D. J. Gross and A. Neveu, Phys. Rev. D **10**, 3235 (1974), URL <https://link.aps.org/doi/10.1103/PhysRevD.10.3235>.
- ²⁰ K. Slagle, Y.-Z. You, and C. Xu, Phys. Rev. B **91**, 115121 (2015).
- ²¹ Y.-Y. He, H.-Q. Wu, Y.-Z. You, C. Xu, Z. Y. Meng, and Z.-Y. Lu, Phys. Rev. B **94**, 241111 (2016), URL <https://link.aps.org/doi/10.1103/PhysRevB.94.241111>.
- ²² Y.-Z. You, Y.-C. He, C. Xu, and A. Vishwanath, Phys. Rev. X **8**, 011026 (2018), URL <https://link.aps.org/doi/10.1103/PhysRevX.8.011026>.
- ²³ Y.-Z. You, Y.-C. He, A. Vishwanath, and C. Xu, Phys. Rev. B **97**, 125112 (2018), URL <https://link.aps.org/doi/10.1103/PhysRevB.97.125112>.
- ²⁴ V. Ayyar and S. Chandrasekharan, Phys. Rev. D **93**, 081701 (2016), URL <https://link.aps.org/doi/10.1103/PhysRevD.93.081701>.
- ²⁵ S. Catterall, Journal of High Energy Physics **2016** (2016), ISSN 1029-8479, URL [http://dx.doi.org/10.1007/JHEP01\(2016\)121](http://dx.doi.org/10.1007/JHEP01(2016)121).
- ²⁶ V. Ayyar and S. Chandrasekharan, Journal of High Energy Physics **2016** (2016), ISSN 1029-8479, URL [http://dx.doi.org/10.1007/JHEP10\(2016\)058](http://dx.doi.org/10.1007/JHEP10(2016)058).
- ²⁷ V. Ayyar and S. Chandrasekharan, Phys. Rev. D **91**, 065035 (2015), URL <https://link.aps.org/doi/10.1103/PhysRevD.91.065035>.
- ²⁸ Y. BenTov, Journal of High Energy Physics **2015** (2015), ISSN 1029-8479, URL [http://dx.doi.org/10.1007/JHEP07\(2015\)034](http://dx.doi.org/10.1007/JHEP07(2015)034).
- ²⁹ T. Kanazawa, Journal of High Energy Physics **2015** (2015), ISSN 1029-8479, URL [http://dx.doi.org/10.1007/JHEP10\(2015\)010](http://dx.doi.org/10.1007/JHEP10(2015)010).
- ³⁰ S. Catterall, *Chiral lattice theories from staggered fermions* (2020), 2010.02290.
- ³¹ S. Catterall, G. C. Toga, and N. Butt, *Symmetric mass generation for kähler-dirac fermions* (2021), 2101.01026.
- ³² Y.-Z. You and C. Xu, Physical Review B **91** (2015), ISSN 1550-235X, URL <http://dx.doi.org/10.1103/PhysRevB.91.125147>.
- ³³ X.-G. Wen, Physical Review D **88** (2013), ISSN 1550-2368,

- URL <http://dx.doi.org/10.1103/PhysRevD.88.045013>.
- ³⁴ X.-G. Wen, Chinese Physics Letters **30**, 111101 (2013), ISSN 1741-3540, URL <http://dx.doi.org/10.1088/0256-307X/30/11/111101>.
- ³⁵ J. Wang and X.-G. Wen, *Non-perturbative regularization of 1+1d anomaly-free chiral fermions and bosons: On the equivalence of anomaly matching conditions and boundary gapping rules* (2019), 1307.7480.
- ³⁶ J. Wang and X.-G. Wen, Physical Review Research **2** (2020), ISSN 2643-1564, URL <http://dx.doi.org/10.1103/PhysRevResearch.2.023356>.
- ³⁷ S. S. Razamat and D. Tong, *Gapped chiral fermions* (2021), 2009.05037.
- ³⁸ Y.-Z. You, Y. BenTov, and C. Xu, *Interacting topological superconductors and possible origin of 16n chiral fermions in the standard model* (2014), 1402.4151.
- ³⁹ J. Wang and X.-G. Wen, Physical Review D **99** (2019), ISSN 2470-0029, URL <http://dx.doi.org/10.1103/PhysRevD.99.111501>.
- ⁴⁰ V. Gurarie, Phys. Rev. B **83**, 085426 (2011), URL <https://link.aps.org/doi/10.1103/PhysRevB.83.085426>.
- ⁴¹ A. M. Essin and V. Gurarie, Phys. Rev. B **84**, 125132 (2011), URL <https://link.aps.org/doi/10.1103/PhysRevB.84.125132>.
- ⁴² R.-J. Slager, L. Rademaker, J. Zaanen, and L. Balents, Physical Review B **92** (2015), ISSN 1550-235X, URL <http://dx.doi.org/10.1103/PhysRevB.92.085126>.
- ⁴³ Y.-Z. You, Z. Wang, J. Oon, and C. Xu, Phys. Rev. B **90**, 060502 (2014), URL <https://link.aps.org/doi/10.1103/PhysRevB.90.060502>.
- ⁴⁴ X. Chen, Y.-M. Lu, and A. Vishwanath, Nature Communications **5**, 3507 (2014).
- ⁴⁵ G. E. Volovik and V. M. Yakovenko, Journal of Physics: Condensed Matter **1**, 5263 (1989), URL <https://doi.org/10.1088/0953-8984/1/31/025>.
- ⁴⁶ G. E. Volovik, *The Universe in a Helium Droplet* (Oxford University Press, 2003).
- ⁴⁷ Z. Wang, X.-L. Qi, and S.-C. Zhang, Phys. Rev. Lett. **105**, 256803 (2010), URL <https://link.aps.org/doi/10.1103/PhysRevLett.105.256803>.
- ⁴⁸ Z. Wang and S.-C. Zhang, Phys. Rev. B **86**, 165116 (2012), URL <https://link.aps.org/doi/10.1103/PhysRevB.86.165116>.
- ⁴⁹ Z. Wang and S.-C. Zhang, Phys. Rev. X **2**, 031008 (2012), URL <https://link.aps.org/doi/10.1103/PhysRevX.2.031008>.
- ⁵⁰ Z. Bi and T. Senthil, Physical Review X **9** (2019), ISSN 2160-3308, URL <http://dx.doi.org/10.1103/PhysRevX.9.021034>.
- ⁵¹ C.-M. Jian and C. Xu, Physical Review B **101** (2020), ISSN 2469-9969, URL <http://dx.doi.org/10.1103/PhysRevB.101.035118>.
- ⁵² J. T. Chalker and P. D. Coddington, Journal of Physics C: Solid State Physics **21**, 2665 (1988), URL <http://stacks.iop.org/0022-3719/21/i=14/a=008>.
- ⁵³ J. B. Marston and S.-W. Tsai, Phys. Rev. Lett. **82**, 4906 (1999), URL <https://link.aps.org/doi/10.1103/PhysRevLett.82.4906>.
- ⁵⁴ L. Tsui, H.-C. Jiang, Y.-M. Lu, and D.-H. Lee, Nuclear Physics B **896**, 330C359 (2015), ISSN 0550-3213, URL <http://dx.doi.org/10.1016/j.nuclphysb.2015.04.020>.

This figure "fig1new2.JPG" is available in "JPG" format from:

<http://arxiv.org/ps/2103.15865v1>

This figure "fig2new2.JPG" is available in "JPG" format from:

<http://arxiv.org/ps/2103.15865v1>

This figure "fig3new2.JPG" is available in "JPG" format from:

<http://arxiv.org/ps/2103.15865v1>

This figure "fig4new2.JPG" is available in "JPG" format from:

<http://arxiv.org/ps/2103.15865v1>

This figure "fig5new2.JPG" is available in "JPG" format from:

<http://arxiv.org/ps/2103.15865v1>

This figure "fig6new2.jpg" is available in "jpg" format from:

<http://arxiv.org/ps/2103.15865v1>

This figure "fig7new2.JPG" is available in "JPG" format from:

<http://arxiv.org/ps/2103.15865v1>